Frequency-Dependent Characterization of Bulk and Ceramic Bypass Capacitors

Istvan Novak, Jason R. Miller
SUN Microsystems, Inc.
One Network Drive, Burlington, MA 01803
tel: (781) 442 0340, fax: (781) 442 0402
e-mail: istvan.novak@sun.com, jason.r.miller@sun.com

Abstract:
Power distribution networks (PDN) use various kinds of capacitors to create the required impedance profile and to suppress noise. The simple model of bypass capacitors is a series R-L-C network with frequency independent parameters. The paper gives measured data for radial-lead and D-size bulk capacitors and 1210, 0508, 0402 two-terminal and 0612 eight-terminal ceramic capacitors, showing the extraction procedure and frequency dependent data of all three parameters. Various physical contributors to the frequency dependencies are identified. Test fixture geometries are given with their electrical characterization, and capacitors with horizontal and vertical plate mounting are compared.

I. Introduction

Often times the *Power Distribution Network* (PDN) is designed and validated in the frequency domain. The most frequently used elements in PDN are the bypass capacitors. They range from polymer and electrolytic as well as tantalum and niobium capacitors with thousands of microfarad capacitance, to ceramic capacitors in the pF capacitance range. By neglecting the parallel DC leakage current, which is seldom a concern in the overall PDN impedance profile, the typical model of a bypass capacitor is a series R-L-C network, creating a *series resonance frequency* (SRF), where the impedance magnitude of the part equals its *equivalent series resistance* (ESR). Beyond the SRF, the impedance is dominated by inductance, usually called as *equivalent series inductance* (ESL). In first approximation, all three parameters, C, R (or ESR) and L (or ESL) are independent of frequency. Upon closer inspection, all three parameters also depend on frequency to various degrees and for different reasons, creating the need to understand and analyze the C(f), R(f) and L(f) functions. More importantly, some of the parameters, notably L(f) and to a lesser degree, also R(f), show a frequency dependence intermingled with a dependence upon the geometry of user-defined external connections.

In this paper we give measurement data and extracted C(f), R(f) and L(f) functions of different bypass capacitors, based on measurement and extraction procedures detailed in [1], and describe several test fixtures which can be used for generic component-parameter extraction. We use the equivalent circuit of Figure 1.a for frequency ranges and geometries where the fixture capacitance can be neglected. This is the case for parts with large capacitance, measured at low and medium frequencies in a small-size fixture. The equivalent circuit of Figure 1.b is used, when the fixture capacitance should not be neglected: parts with lower capacitance, measured up to higher frequencies, which includes the resonance frequency between the fixture capacitance and part's inductance. Including the Cp fixture capacitance, all parameters are treated as variables of frequency during the measurement and extraction process. The same measurement and extraction processes can be used to measure component parameters under non-zero DC bias voltage conditions and at different temperatures, though such data is not presented here.

II. Limitations of frequency independent models

To illustrate the frequency dependency of parameters, we first look at the measured impedance profile of a 0508-size reverse-geometry 4.7uF two-terminal bypass capacitor as an example. The measured part does not have the lowest ESR available today, nor has it the highest capacitance in its case size, and it did not have the most aggressive mounting geometry either. The part was mounted on a small piece of multiplayer *printed circuit board* (PCB), and its impedance was measured on the planes using a close-by pair of test vias. There are several different test fixtures in this paper: this is referred to as Test Fixture A. It had 1"x0.14" plane shapes and capacitor pads with two vias per pad. The fixture's photo, cross section and geometry details are shown in

Figure 2. The measured impedance profile is shown in Figure 3. The impedance was measured over the 100 Hz to 1.8 GHz frequency range with two different instruments, covering the 100 Hz to 10 MHz and 100 kHz to 1800 MHz frequency ranges, respectively, and the chart contains two independently obtained magnitude and phase curves. For the magnitude traces, different colors indicate the two frequency ranges: green for the low frequency measured data and blue for the higher frequency measured data.

The impedance plot shows a series resonance frequency at 2.65 MHz (series resonance of C and L of the equivalent circuit of Figure 1(a), or Cs and L of Figure 1(b) and a *parallel resonance frequency* (PRF) between the capacitor's inductance and the static plane capacitance at 682 MHz (parallel resonance of Cp and L of the equivalent circuit of Figure 1(b). At SRF, the impedance reading is 6.48 mOhms, which may be used as the first estimate of ESR . From the 100 Hz impedance point, the capacitance was estimated to be Co= 4.94 uF. Assuming that at SRF Co resonates with ESL, the L(SRF) estimate is 729 pH. The plane capacitance of the small test fixture was measured at PRF as Cp= 115 pF. Assuming that at PRF ESL resonates with Cp, the L(PRF) estimate becomes 474 pH. Far away from SRF and PRF, the slopes on the Bode plot appear to be linear, suggesting frequency independent capacitance and inductance.

However, by extracting the C(f), L(f), and R(f) functions from the measured complex impedance profile, they reveal considerable frequency dependency. Figure 4 shows the extracted C(f) and L(f) parameters. From these curves, C(100Hz) = 4.94 uF, C(SRF) = 4.0 uF or a –19% change; L(SRF) = 870 pH; L(PRF)= 470 pH, or a –46% change. Later we show that C and L can vary significantly more, depending on the part and it's mounting. The frequency dependent real part of impedance (equivalent series resistance) is shown in Figure 5, separately for the sample together with Test Fixture A and Test Fixture A with shorted capacitor pads. These curves were also obtained with two different instrumentations, one covering lower and the other covering higher frequencies. Figure 6 shows the percentage error of impedance magnitude between the measured (Figure 3) and estimated/simulated curves with four possible combinations of constant, frequency independent C, L and R values. No matter how we pick the constant values, the frequency independent model results in large error.

III. Procedure to extract frequency-dependent parameters

It is known [2] that above the series resonance frequency of the mounted part, the size and shape of the current loop inside the capacitor changes and therefore as frequency goes up resistance increases and inductance decreases. For the same reason, capacitance above SRF can be expected to drop as well. However, being dominated by the inductive reactance, the dropping capacitive reactance with increasing frequency creates a negligible contribution of the total impedance, therefore this effect will not be considered further. It was found empirically that the magnitude and slope of change in resistance and inductance above SRF depends on ESR(SRF) and on the relative dimensions of the capacitor body, pads, vias and closest plane(s). The lower the ESR(SRF) value, and the more aggressive the mounting, aiming for lower overall inductance, the bigger percentage change it will create in the resistance and inductance functions with frequency. Because the R(f) and L(f) functions also depend on the application geometry, it is important to measure the part in a fixture, with pad, via and plane geometries being similar to the actual usage. This way the measured complex Z_{DUT} impedance will reflect both the device under test and the fixture, and we address the selection of fixture geometry and the de-embedding of fixture parameters later in this paper. We can de-embed the resistance of fixture, but not its inductance: only an 'added inductance' can be defined, which is characteristic to the capacitor body.

After the proper calibration, the two-port VNA measurement yields the real and imaginary part of the unknown Z_{DUT} impedance through the following formulas [1]:

$$\mathrm{Re}(Z_{DUT}) = 25 * \frac{\mathrm{Re}(S_{21}) * (1 - \mathrm{Re}(S_{21})) - \mathrm{Im}(S_{21})^2}{(1 - \mathrm{Re}(S_{21}))^2 + \mathrm{Im}(S_{21})^2}$$

$$\mathrm{Im}(Z_{DUT}) = 25 * \frac{\mathrm{Im}(S_{21}) * (1 - \mathrm{Re}(S_{21})) + \mathrm{Re}(S_{21}) * \mathrm{Im}(S_{21})}{(1 - \mathrm{Re}(S_{21}))^2 + \mathrm{Im}(S_{21})^2}$$

(Note: these formulas in [1] had the second closing brackets in the nominators accidentally missing).

Extracting capacitance versus frequency: Using a small fixture, we can make sure that its static plane capacitance is much smaller than the capacitance of the DUT. The fixture (Test Fixture A) for taking data for Figure 3 had a Cp = 115 pF capacitance at PRF, allowing us to measure DUT capacitances as low as 10nF without introducing more than one percent error due to fixture capacitance. We assume that below the series resonance frequency, the imaginary part of the measured impedance, $\mathrm{Im}\{Z_{DUT}\}$ comes from the DUT capacitance. In reality, anywhere below the parallel resonance frequency, $\mathrm{Im}\{Z_{DUT}\}$ is the sum of the capacitive and inductive reactances. Far below or above the series resonance frequency, the capacitance or inductance dominates and the other can be neglected. Close to the series resonance frequency, assuming that L(f) does not jump suddenly, we can apply a correction to the extracted C(f) function by using an L(SRF) estimate, which extends the validity of C(f) extraction to and slightly beyond SRF. Extracted L(f) functions in this paper indicate that the inductance, in fact, does stay relatively constant around SRF and starts to drop noticeably only at two or three times higher frequencies.

Figure 7 shows C(f) extracted from the complex data of Figure 3 on an extended scale, with and without applying correction for L(SRF). With no correction for L(SRF), there is an increasing error of the extracted capacitance value, which seemingly increases the capacitance. By applying the correction for L(SRF), the capacitance-frequency curve follows its lower-frequency trend and the trace extends smoothly up to SRF. The estimate of the capacitance versus frequency function thus becomes:

$$C(f) = -\frac{1}{2\pi f\left(\mathrm{Im}\{Z_{DUT}\} - \omega L(SRF)\right)}$$

Note that above SRF, the C(f) curve may have an increasing error if L(f) changes considerably, but the impedance having been dominated by inductance, the capacitance versus frequency function above SRF is of much less interest. Below SRF, the frequency dependence of the capacitance is believed to come from the capacitor's construction, as well as from variations of the effective dielectric constant of the dielectric material.

Extracting inductance versus frequency: Above the series resonance frequency, but below the parallel resonance of static fixture capacitance and capacitor inductance, the imaginary part of Z_{DUT} is dominated by inductance. If we simply invert $\mathrm{Im}\{Z_{DUT}\}$ to calculate L(f), the curve shows an increasing negative error close to SRF and increasing positive error close to PRF. This is shown by the uncorrected curve of Figure 8, which uses the data from our first example: a 4.7uF 0508 capacitor mounted on Test Fixture A. Knowing the C_p fixture capacitance, and having an estimate on the series capacitance of device under test at SRF, C_s(SRF), we can compensate for both resonances, by applying the formula:

$$L(f) = \frac{\mathrm{Im}\{Z_{DUT}\} + \dfrac{1}{2\pi f C_S(SRF)}}{2\pi f\left(1 + 2\pi f\, C_P\, \mathrm{Im}\left(Z_{DUT}\right)\right)}$$

The above formula assumes that the series and parallel resonances are sufficiently apart along the frequency axis, which is usually the case. Note that even if the fixture capacitance is small enough that we can ignore it for the calculation of DUT capacitance, it is still necessary to compensate for it if we want to extend the extraction of inductance up to the parallel resonance frequency.

The corrected curve in Figure 8 is valid over almost three decades of frequency, whereas without these two compensations, the extracted inductance hardly covers one decade of frequency with reasonable accuracy. The inductance curve represents the entire loop formed by the pads, vias, planes and the capacitor body itself. Note that the curve extends smoothly above and below the two resonance frequencies: the only artifact is a spike in a very narrow frequency band around the parallel resonance frequency.

We can also define and obtain the Added Inductance of the capacitor body, beyond the $L_{sh\text{-}fx}$(f) inductance of the fixture with shorted pads:

$L_{Added}(f) = L(f) - L_{sh\text{-}fx}(f)$

The trace of Added Inductance in Figure 9 shows that this particular 0508 capacitor body, together with the given pads and vias, created an extra inductance beyond that of the same fixture, pads and vias, which varies from 300 pH at SRF to about 50 pH at PRF, a six-to-one range.

Extracting resistance versus frequency: As opposed to capacitance and inductance, Real{Z_{DUT}} is not the sum of parameters changing with frequency in opposite ways. However, it is still the sum of the series resistance of the fixture, R_{fx}, and the series and parallel losses R_s and R_p of the capacitor. In the curve of Figure 5, the R_p dielectric loss dominates the slope up to about 100kHz. Above 100kHz, the $R_s + R_{fx}$ conductive loss dominates. Figure 10 shows the deembedding stages: first the shorted fixture is measured, with a shorting strip soldered across the capacitor pads, and its $R_{sh\text{-}fx}(f)$ curve is plotted. The de-embedded resistance (Added Resistance) of DUT becomes

$$R_{Added}(f) = Real\{Z_m(f)\} - R_{sh\text{-}fx}(f)$$

At SRF, the de-embedded ESR(SRF) Added Resistance of DUT is 2.70 mOhms. Note: before de-embedding, our ESR(SRF) estimate was 6.48 mOhms.

Fixture characterization: To complete the above extraction procedure, one also has to obtain the frequency dependent parameters of the test fixture. These parameters include the C_p(PRF) parallel fixture capacitance at the parallel resonance frequency, and the $R_{sh\text{-}fx}(f)$ and $L_{sh\text{-}fx}(f)$ resistance and inductance of the test fixture with the capacitor pads shorted. Extracting Cp appears to be simple; we just measure the capacitance of the bare fixture. However, with most of the fixture materials, especially those which use dielectric materials similar to what are being used in cost-effective volume-production printed-circuit boards, the capacitance is also a function of frequency, therefore we have to measure the fixture capacitance at the particular frequency where we want to use it for fixture correction. This is illustrated in Figure 11, which shows on an expanded vertical scale the extracted capacitance from the impedance measured on bare Test Fixture A. The trace clearly indicates a capacitance decreasing with frequency: approximately 126pF at 1MHz and 108pF at 1GHz, an almost –20% change over three decades of frequency. The straight line in the figure is an exponential approximation (note: the linear-logarithmic scale of the chart transforms the exponential function to a straight line). The approximation formula is:

$$C_{approx}(f) = C_0\left(\frac{f}{a}\right)^b$$

For Test Fixture A, C_0 = 130pF, a = 200kHz, b = -0.022 were used. The shorted test fixture parameters were already shown in Figure 5 (resistance) and Figure 9 (inductance). A 3D solid model was also developed directly from the test board using the board file and stack up. HFSS, a full-wave electromagnetic solver, was used to calculate the S-parameters for the shorted structure at the two probe points from 10 MHz to 1 GHz. The equivalent inductance was then extracted directly from the S-parameter data. The trace of the simulated inductance of shorted Test Fixture A is shown in Figure 12. Figures 13 and 14 show the side view and 3D view of the simulated structure.

IV. Data of various bulk and ceramic capacitors

Bulk capacitors: Figure 15 shows the normalized C(f) curves of four bulk capacitors, labeled A through D. A and B are 1200uF and 1000uF low-ESR radial bulk capacitors, C and D are 330uF and 390uF D-size polymer capacitors. The curves are shown up to their particular SRF. Figure 16 shows the inductance together with the particular fixture for the same four bulk capacitors. Parts A and B used the near site of Test Fixture B (see Figure 17), parts C and D were measured in Test Fixture C (see Figure 18). Capacitor A looses more than half of its capacitance close to SRF, and it had the highest inductance. Capacitor B in the same-size aluminum can exhibits about half of the capacitance drop, and its inductance (together with the fixture) is also about 50% less. Capacitors C and D showed much less capacitance loss below 100kHz, but part C (due to its lower inductance) has a higher SRF, and up to that higher SRF it still looses almost 40% of its capacitance. This was partly offset by the fact that part D had by far the lowest inductance. Parts A, B and C showed very minimal change of inductance over the measured 0.1 to 10MHz frequency range. Part D, however, which comes in a taller version of the D-size package, exhibited more than 2:1 inductance drop. Part C has a face down, low-inductance construction, similar to the one described in [3]. Figures 19 and 20 show the inductance of Fixture B and C,

with near site and far site shorted, respectively. Note that the surface-mount pads of Fixture C with two vias per pad provide a noticeably lower inductance.

Ceramic capacitors

Sample parts E, F and G were 100uF X5R 1210, 1uF X7R 0508 and 0.1uF X7R 0402 ceramic capacitors, respectively. Figure 21 shows their relative capacitance change with frequency, normalized to their nominal capacitance values. Figure 22 shows their inductance versus frequency, together with the test fixture. The three parts had three different test fixtures (not shown here), matching the required pad dimensions for the parts. The 0402-size 0.1uF part (G) was measured with the same via diameter and pad arrangements with two via lengths: 5 mils and 130 mils, in a near site and a far site. Curve for the 100uF part was measured only up to 10 MHz.

Testing the uniqueness of Added Inductance

Some of the capacitor samples were measured in the near site and far site locations of the test fixtures, and their Added Inductances were extracted to see how independent it is from the inductance of shorted fixture with different via lengths leading to the nearest plane. Figure 23 shows the Added Inductance of one bulk capacitor (part A, 1200uF radial) and one ceramic capacitor (part G, 0.1uF 0402). The two test fixtures had pads on both top and bottom, connected to the planes, which were closer to one side. The via lengths for part A (in the near site and far site of Test Fixture B) were 5-mil and 57-mil, for part G 5-mil and 130-mil. Note that the added inductance of the part is fairly independent of the via length, and therefore it is a good measure of the 'goodness' of capacitor.

Multi-terminal capacitors

Multi-terminal capacitors are becoming popular because of their lower inductance. Three eight-terminal 0612-size capacitors from three different vendors were measured and evaluated. Throughout Figures 24-27, labels A, B and C refer to a 2.2uF X7R, 1uF X7R, and 4x1uF X7R part, respectively. Parts A and B were single capacitors with eight terminals, part C was a capacitor array with four independent capacitors in the package. The three parts were measured using the same Test Fixture D, defined in Figure 28. The fixture had a pair of planes of size 1"x0.64", the capacitor pads and test vias were separated by an x=0.5" y=0.25" distance, and were connected to a pair of planes with 2-mil dielectric separation, 2.8 mils below the surface. The capacitor pads were connected to the L2-L3 planes with 8-mil blind vias located inside the pads.

Figure 24 compares the impedance magnitudes in the 100kHz-100MHz frequency range. Figure 25 shows the percentage change of extracted capacitance in the frequency range of 1kHz and 1MHz, normalized to each part's nominal capacitance value. The three parts show similar rate of capacitance change with frequency: over three decades, the capacitance drops smoothly by 7-8%. Figure 26 compares the extracted Added Resistance values of the parts in the 100kHz-100MHz frequency range. When compared to the impedance-magnitude plots in Figure 24, the following conclusions can be drawn. The self resonant frequency of part C is 10MHz, whereas the frequency of minimum added resistance is 3MHz. From 3MHz to 10MHz the added resistance of the part increases from 3.5 milliohms to 4 millohms. Between 10 and 25MHz, the added resistance rises to 10 milliohms. Similarly, for part B, SRF is at 5MHz, the frequency where the added resistance is at its minimum is 2.5MHz. The lowest Q and highest added resistance come with part A, where there is no noticeable difference between its SRF and frequency of minimum added resistance. Part A exhibits the smoothest shape of added resistance curve, with no sudden increase above SRF. Note also that above 40MHz the added resistance curves of the three parts are almost identical.

In Figure 27, the Added Inductances of the parts are compared in the 1MHz to 1GHz frequency range. The inductance curves have to be evaluated together with the cross section pictures in Figure 29, showing the outer and internal geometry of three capacitors of the same makes as samples A, B and C. Thanks to corrections for C(SRF) and Cp(PRF), the usable frequency range of inductance curves extends down to a few MHz and up to about 1GHz. Note that at and below SRF, parts A and B have about 100pH added inductance, whereas part C has 150pH added inductance. The fixture and mounting was the same for all three parts, and Figure 29 shows that the total body height was also about the same. Parts A and B were single-piece capacitors,

with continuous horizontal capacitor plates over the eight connecting terminals. However, part C had four individual capacitors in the same body, resulting in four narrower strips of capacitor plates arching over the terminal pads, thus resulting in higher inductance. For all three parts the Added Inductance stays at about the same value up to 2-3 times the series resonance frequency. This is the frequency range where the Added Resistance already rises significantly. Beyond this point, where the strong change of Added Resistance stops, the inductance starts to drop: the higher the Q of the particular part, the steeper is the drop of inductance.

Above about 40MHz, where the three Added Resistance curves overlap, the Added Inductance curves track with approximately constant (frequency independent) offsets. The lowest inductance comes with part B, which has the thinnest cover thickness on the bottom of capacitor (middle photo of Figure 29). The cross section of part A reveals a much thicker cover, resulting in its higher inductance at high frequencies. Part B and C have similar cover thickness, and they show about the same drop of inductance in the transition region. But having four separate narrower strips in part C, its inductance stays above the other two over the entire measured frequency range. The inductance of the fixture with a shorting strip over all eight pads was 130pH at 100MHz.

In the SRF to PRF frequency range, the added inductance of all three parts drop significantly: for part A it drops from 100pH to 50pH or a 2:1 decrease, for part B it drops from 100pH to 30pH or a 3:1 decrease, and for part C it drops from 150pH to 50pH or a 3:1 decrease.

Vertical orientation of capacitor plates

Secondary resonance and change of parameters with frequency in multi-layer ceramic capacitors have been known in the microwave industry. To reduce secondary resonances, RF circuits sometimes use vertical mounting of the capacitor body such that the multiple capacitor plates are perpendicular to the PCB planes. With the regular form factor of ceramic bypass capacitors, this means the capacitor should stand on its narrower side, raising reliability concerns if accidentally pressure is applied sideways to the part. Ceramic capacitors today approach several hundred uF values in 1810 and 1210 case styles, and 10-22uF in a 0805 case, and 1uF in 603 size. This usually requires an increased height of the part, often resulting in an approximately square side view. The increased number of capacitor plates comes with lower ESR, which in turn results in higher variation of resistance and inductance with frequency.

The square side view has two consequences: with no marking on most ceramic capacitors, if the part accidentally flips during the automated assembly process, it cannot be easily caught by visual inspection. Second, the equal width and height removes the reliability concern from a part mounted with vertical plates on purpose.

Figures 30 through 32 show the results with ten samples of 220uF X5R 1210-size ceramic capacitors. The photo on the left of Figure 33 shows that the width and height of the parts are almost equal. All ten samples were measured in Test Fixture E, without soldering, each sample in both horizontal and vertical orientation. The fixture geometry is shown on the right in Figure 33. The solder-less connection was achieved by applying uncured silver-filled epoxi to the pads, and the samples were pushed onto the pads with a plastic rod during measurement. Figures 30, 31 and 32 show the impedance magnitude, added resistance and added inductance, respectively. The figures show side-by-side the data taken with horizontal mounting (on the left) and vertical mounting (on the right). Each figure has three traces, corresponding to the minimum, average and maximum readings among the ten samples.

The impedance magnitude curves of Figure 30 have zoomed scale around the 200kHz series resonance frequency. The extracted capacitance curves for the parts (not shown here) did not change with the orientation. The impedance magnitude curves with horizontal mounting show a secondary resonance at 600kHz, while with vertical mounting the impedance plots are smooth above SRF. Note that these curves in Figure 31 show the impedance together with the fixture. The Added Resistance curves have relatively little variation around SRF. With horizontal mounting, the Added Resistance rises sharply between 400 and 600kHz. With vertical mounting, the Added Resistance rises slowly and smoothly with frequency. The mounting orientation has the most dramatic effect on the frequency dependence of Added Inductance. With horizontal mounting, the inductance stays at around 1.5nH up to 500kHz and it drops about a full nanohenry between 500 and 600kHz. With vertical mounting, the low-frequency inductance stays in the range of 600 to 800 pH. At high frequencies,

vertical mounting comes with a slightly higher inductance, which is supposedly due to the thicker cover on the capacitor's side.

V. Conclusions

It is shown that bulk and ceramic bypass capacitors may exhibit up to –60% loss of capacitance from low frequencies up to SRF. Measured data indicates that Added Resistance and Added Inductance vary more with frequency for higher-Q parts. Added Inductance may drop by a factor of two to three between SRF and PRF. It was shown that vertical orientation of capacitor plates remove secondary resonances without significantly increasing inductance. Inductance and resistance should be measured in fixtures having stackup and construction similar to the application geometry [4]. Different test fixture geometries were described and their characteristics measured.

Acknowledgement

The authors wish to thank Deborah Foltz, Merle Tetreault, Eric Blomberg, of SUN Microsystems, for their contributions to the test fixtures.

References

[1] I. Novak, "Frequency-Domain Power-Distribution Measurements – An Overview," Part I in HP-TF2, "Measurement of Power Distribution Networks and their Elements", DesignCon East, June 23, 2003, Boston, MA

[2] L.D.Smith, D.Hockanson, K.Kothari, "A Transmission-Line Model for Ceramic Capacitors for CAD Tools Based on Measured Parameters," Proc 52nd Electronic Components & Technology Conference, San Diego, CA., May 2002, pp.331-336

[3] Michihiro Shirashige, Keiji Oka, Kazuto Okada, "New Structure 1608 Size Chip Tantalum Capacitor - 6.3WV 1uF -with Face-down Terminals for Fillet-less Surface Mounting," Proc 51st Electronic Components & Technology Conference, Orlando, FL., May 2001

[4] Michael J. Hill, Leigh Wojewoda, "Capacitor Parameter Extraction – Techniques and Challenges," Intel Technology Symposium, Fall 2003

Figure 1: Lumped equivalent circuit of bypass capacitors with their parallel DC leakage resistance neglected. Figure 1(a) is valid for low and medium frequencies, (b) is good for higher frequencies. All parameters are treated as variables of frequency.

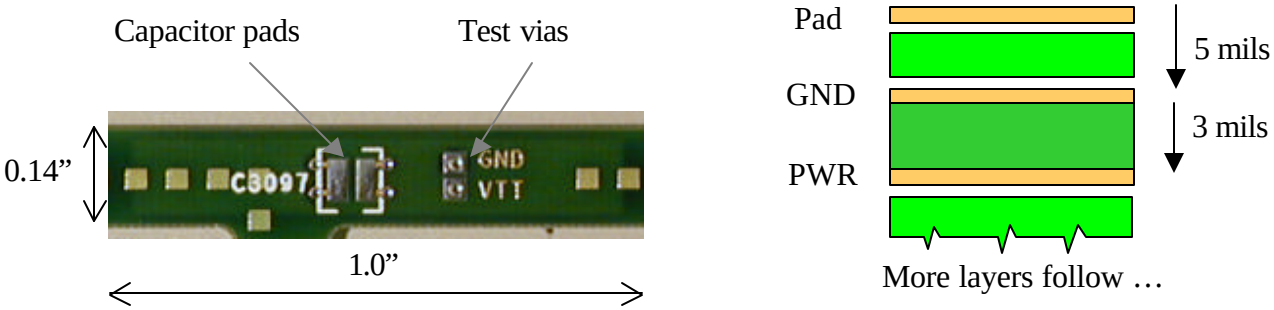

Figure 2: Top view, horizontal geometry and pad/via arrangement of Test Fixture A. On the right, the allocation of the 1"x0.14" planes is shown with their vertical geometry. The capacitor pads have two vias for each pad, with a 50-mil center-to-center spacing and 12-mil finished diameter.

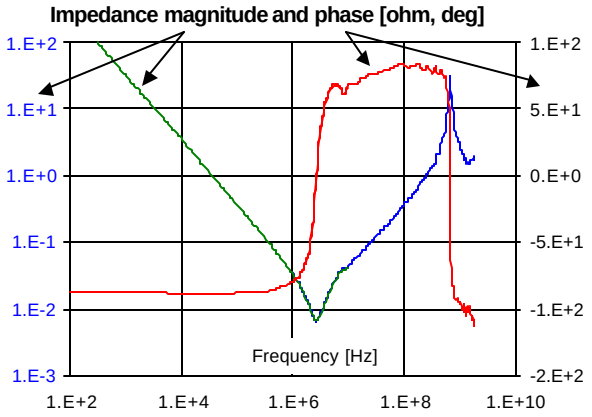

Figure 3: Impedance magnitude and phase of a 4.7uF 0508 ceramic capacitor on Test Fixture A.

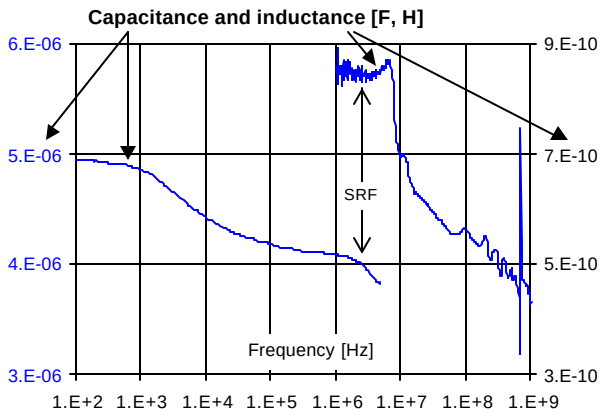

Figure 4: C(f) and L(f) parameters extracted from data of Figure 3. Note the variations with frequency

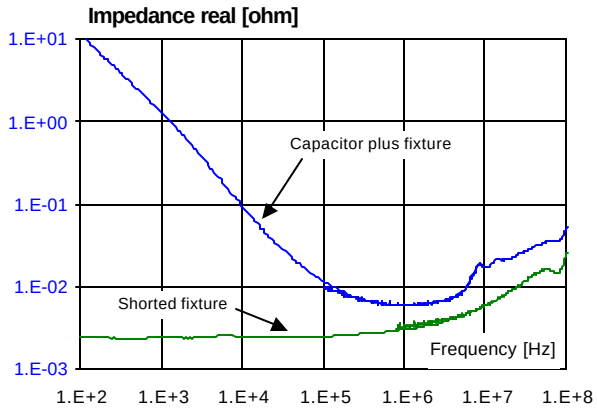

Figure 5: R(f) from data of Figure 3 (Capacitor plus Test Fixture A) and shorted fixture without capacitor.

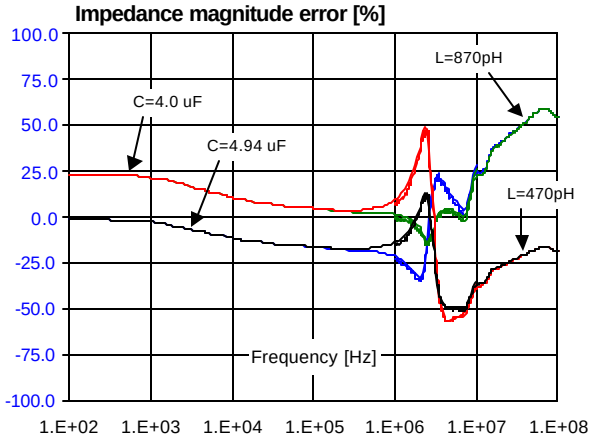

Figure 6: Percentage error of estimated impedance magnitude with constant C, L and R= 6.48 mOhms.

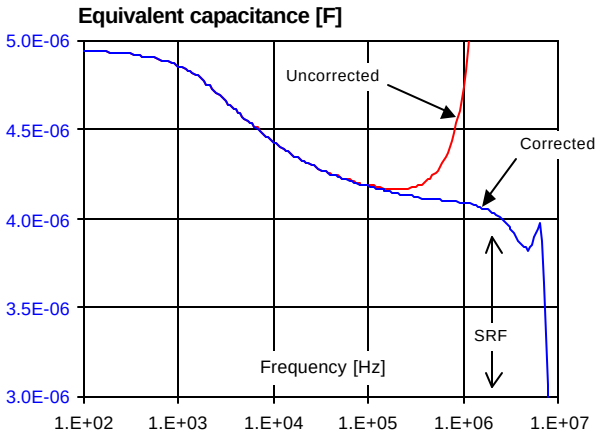

Figure 7: C(f) extracted from impedance of Figure 3, with and without correcting for L(SRF).

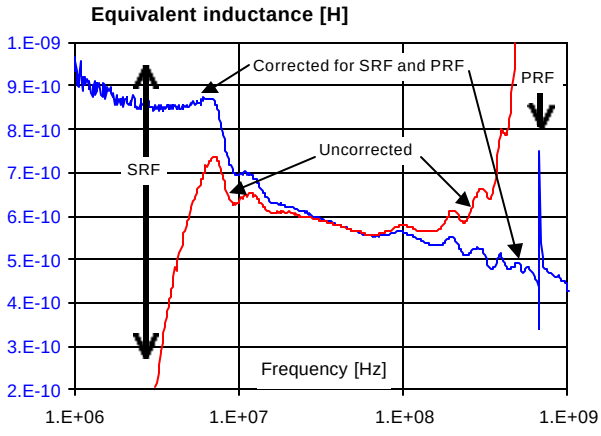

Figure 8: L(f) extracted from impedance of Figure 3, with and without correcting for SRF and PRF.

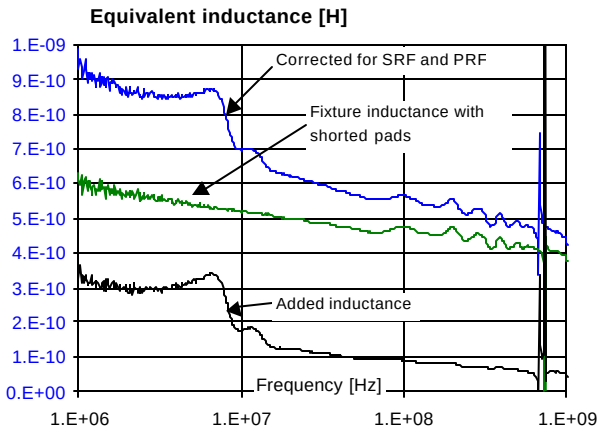

Figure 9: Components of L(f), using data of Figure 3, including inductance of shorted Test Fixture A.

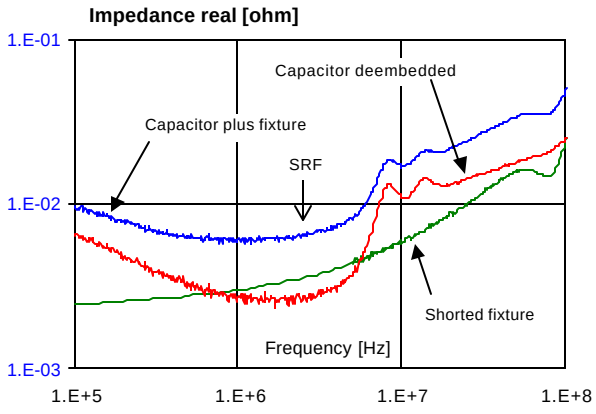

Figure 10: De-embedded real part of impedance, Added Resistance from capacitor data from Figure 5.

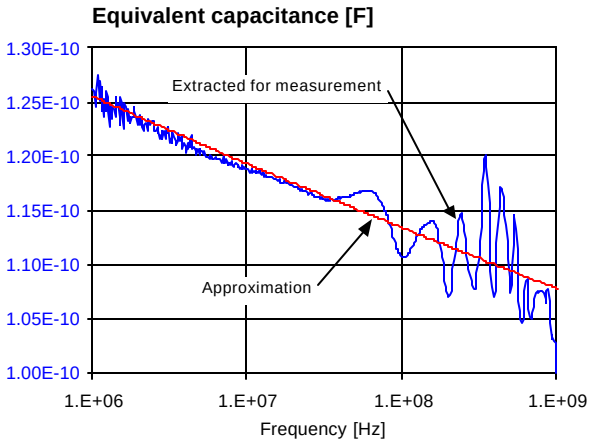

Figure 11: Extracted capacitance $C_p(f)$ of bare Test Fixture A, and exponential approximation curve.

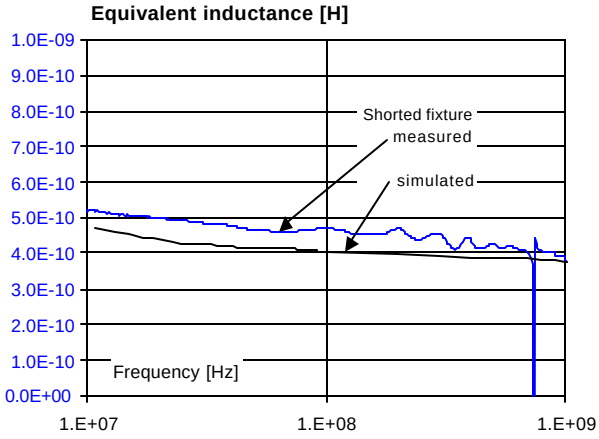

Figure 12: Measured and simulated inductance of shorted Test Fixture A.

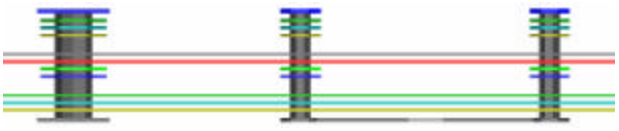

Figure 13: Side view of metal objects in Test Fixture A. Capacitor pads are shown on bottom.

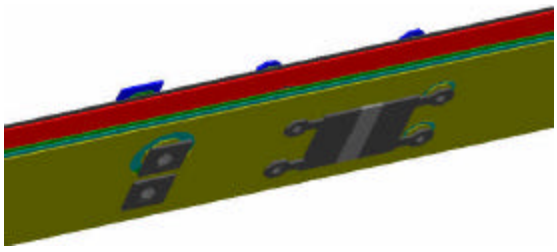

Figure 14: 3D view of shorted Test Fixture A. Picture generated by Ansoft HFSS.

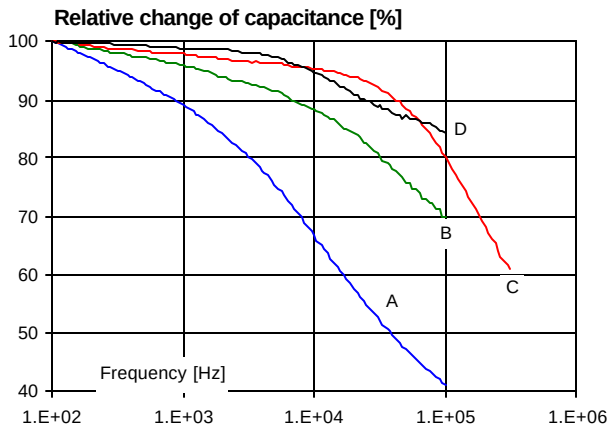

Figure 15: Normalized C(f) curves for two radial bulk (A, B), and two D-size bulk capacitors (C, D).

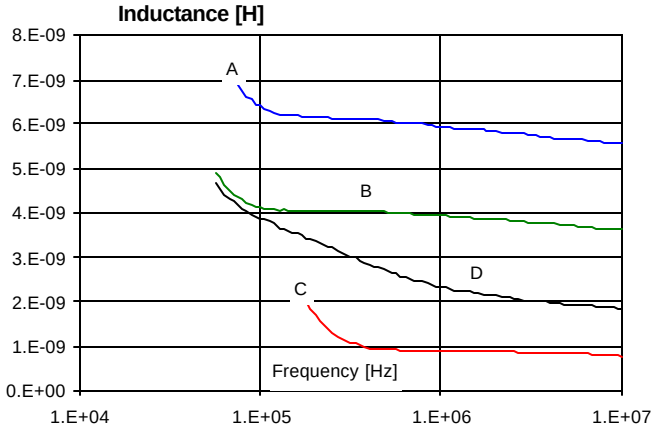

Figure 16: L(f) curves of the bulk capacitors from Fig. 15. A, B and C, D used same fixture, respectively.

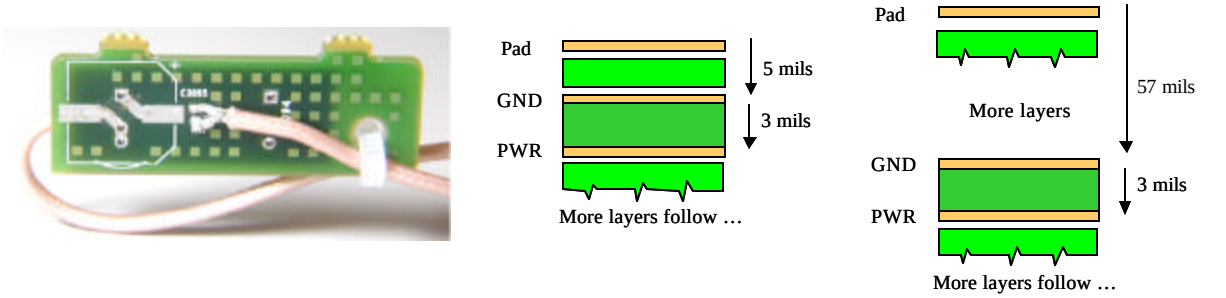

Figure 17: Photo of Test Fixture B on the left, showing soldered cable connections attached to the opposite sides of test through holes. The fixture has two combination sites for various capacitor bodies, one set on either side. The capacitor pads on one side are close to the planes, its corresponding stackup is shown in the middle. This is called the near site of the fixture. The pads on the other side of the board are further away from the planes, with a stackup shown on the right, called the far site of the fixture. The plane shapes are 1065x415 mils.

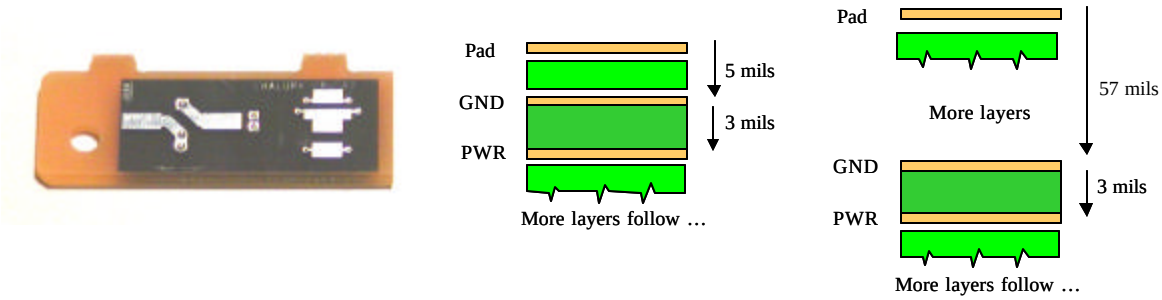

Figure 18: Photo of Test Fixture C on the left. This fixture used the capacitor pads shown on the right half of the fixture, one set on either side, mirrored, and connected to the planes with the same vias. The capacitor pads on one side are close to the planes, its corresponding stackup is shown in the middle. This is called the near site of the fixture. The pads on the other side of the board are further away from the planes, with a stackup shown on the right. This is called the far site of the fixture. The regular D-size part connected to the outer two pads only. The face-down D-size part used all three connections. The size of plane shapes is 1065x415 mils.

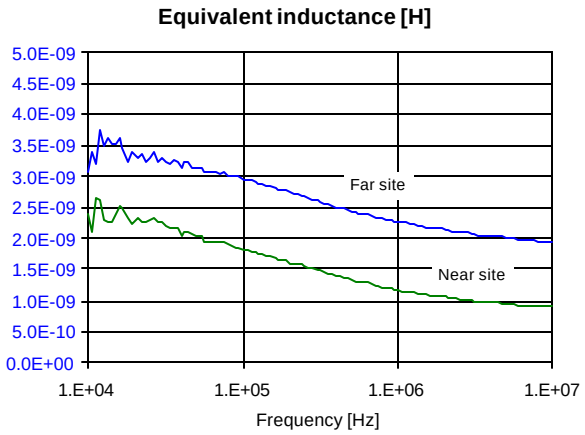

Figure 19: Inductance of Test Fixture B with near site and far site shorted, respectively.

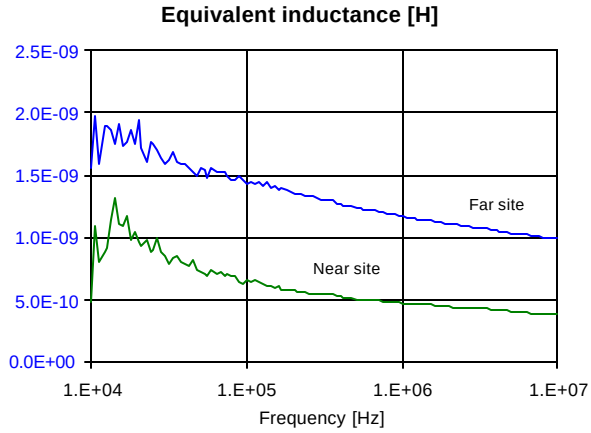

Figure 20: Inductance of Test Fixture C with near site and far site shorted, respectively.

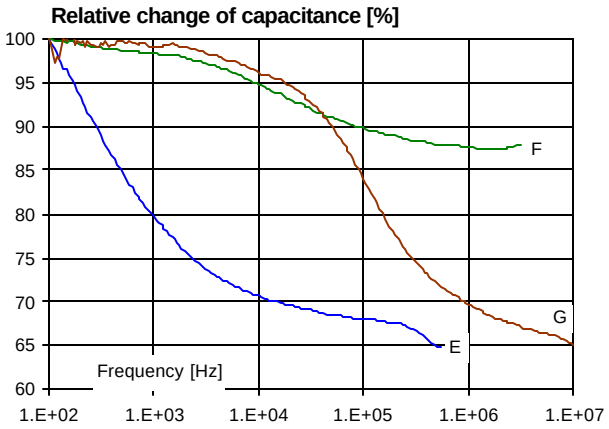

Figure 21: Percentage drop of three ceramic capacitor samples.

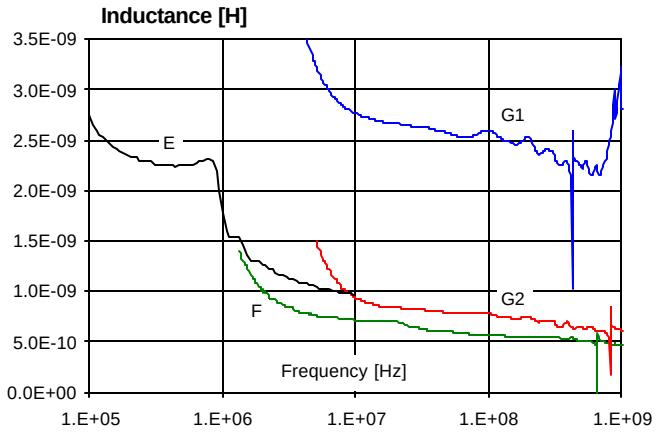

Figure 22: Inductance versus frequency (with fixture) of the three capacitor samples shown in Figure 21

.

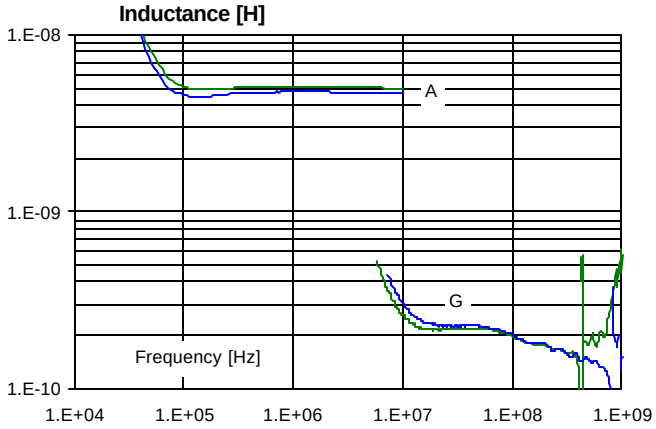

Figure 23: Added inductance of bulk capacitor A and ceramic capacitor sample G extracted from near-site and far-site pad location data.

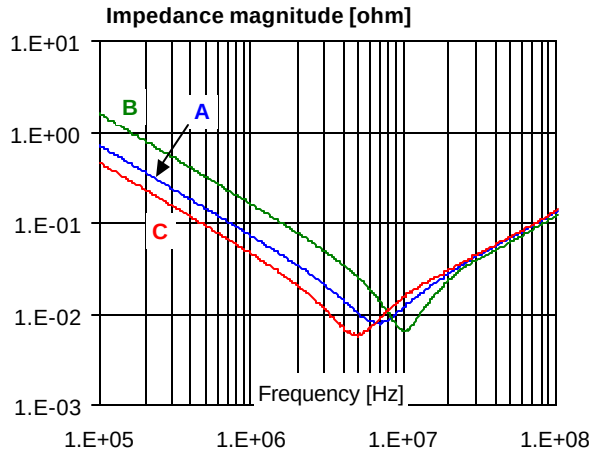

Figure 24: Measured impedance magnitude of three eight-terminal, 1206-size capacitors in Test Fixture D.

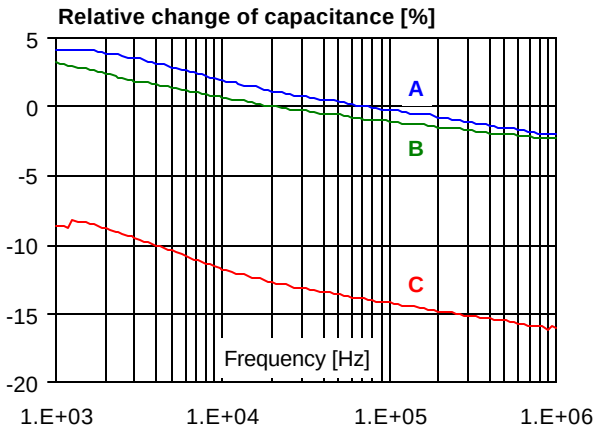

Figure 25: Relative C(f) values of the three parts from Figure 24, referenced to nominal value.

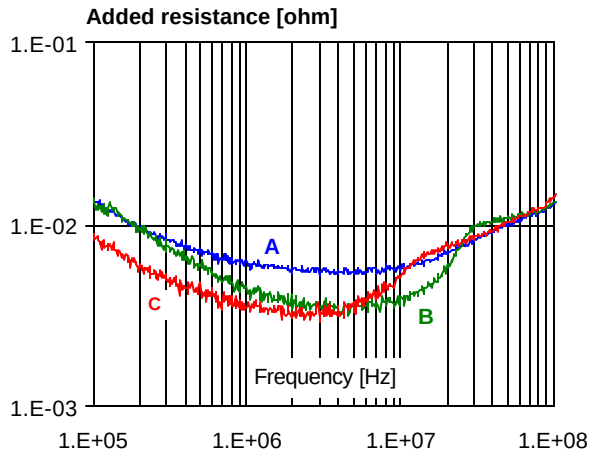

Figure 26: Added Resistance of capacitors from Figure 24.

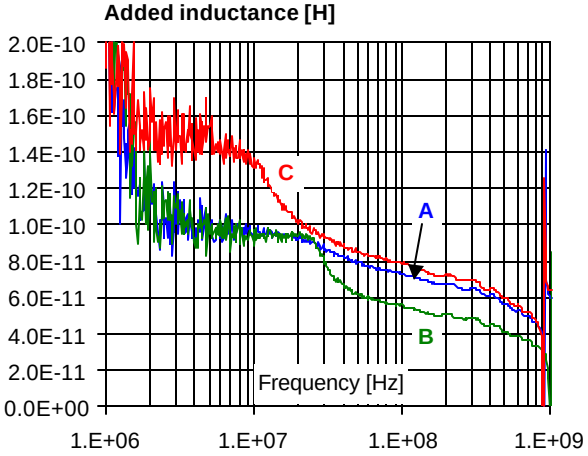

Figure 27: Added Inductance of the three capacitors from Figure 24.

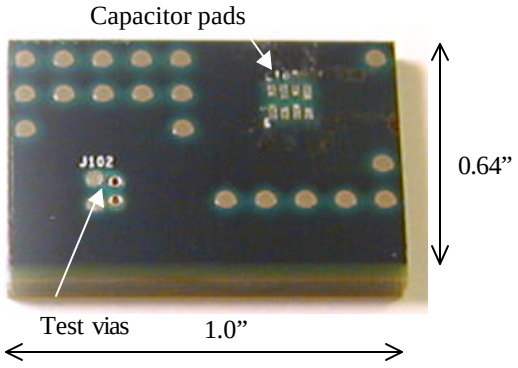

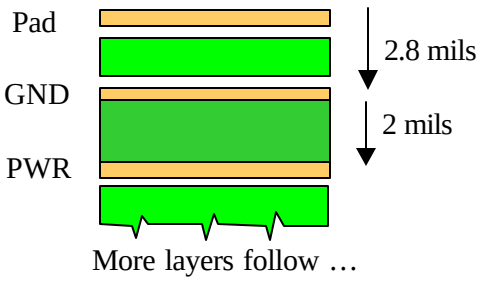

Figure 28: On the left: top view, dimensions and location of capacitor pads and test vias in Test Fixture D. On the right: cross section and vertical geometry of nearest planes in Test Fixture D

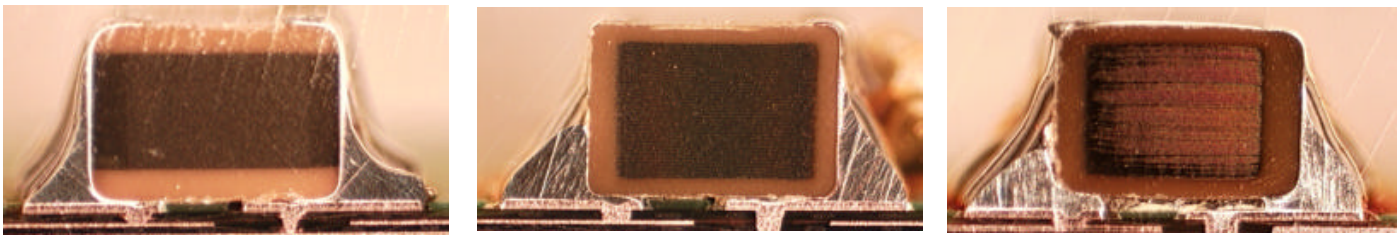

Figure 29: Cross sections of eight-terminal capacitors of makes A, B, and C (from left to right).

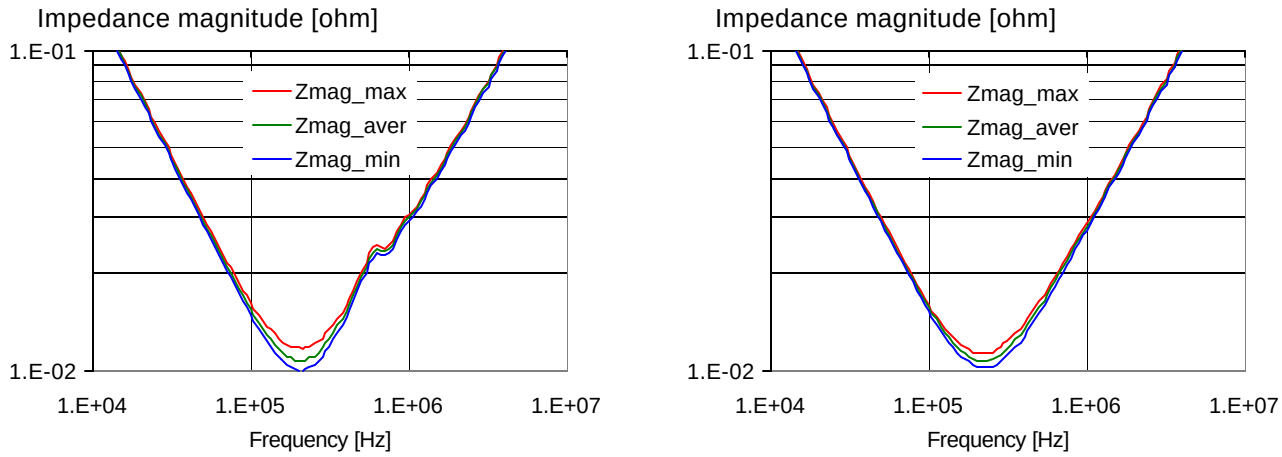

Figure 30: Impedance magnitude statistics of ten samples of 220uF 1210 X5R ceramic capacitors in Test Fixture D. On the left: horizontal mounting. On the right: vertical mounting.

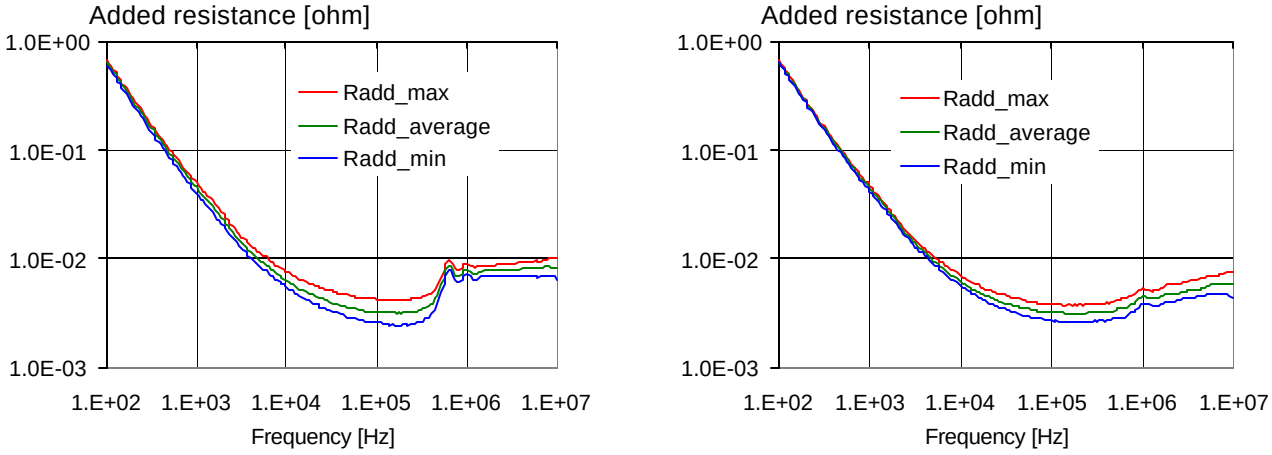

Figure 31: Added resistance statistics of ten samples of 220uF 1210 X5R ceramic capacitors in Test Fixture D. On the left: horizontal mounting. On the right: vertical mounting.

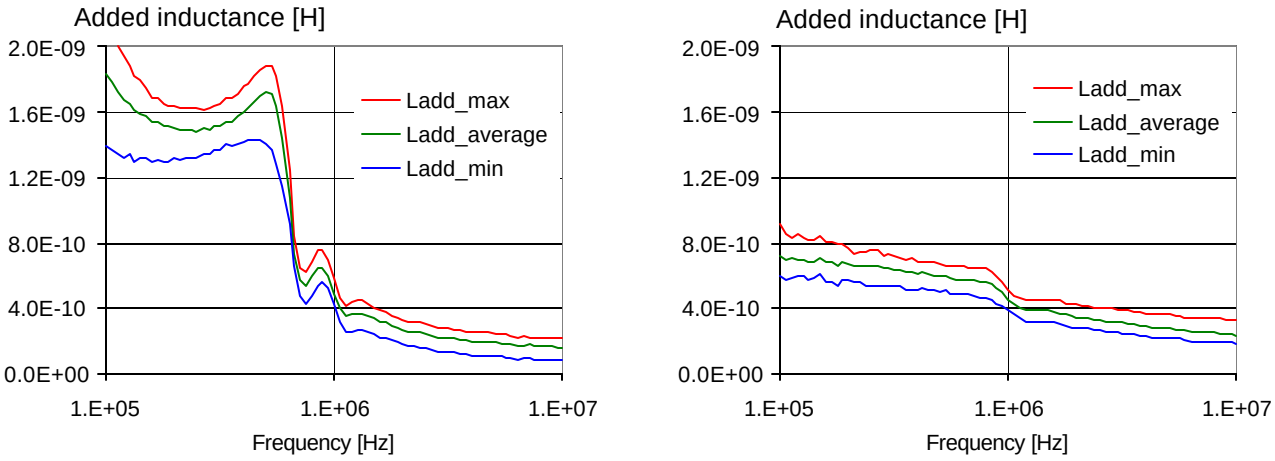

Figure 32: Added inductance statistics of ten samples of 220uF 1210 X5R ceramic capacitors in Test Fixture E. On the left: with horizontal mounting. On the right: with vertical mounting.

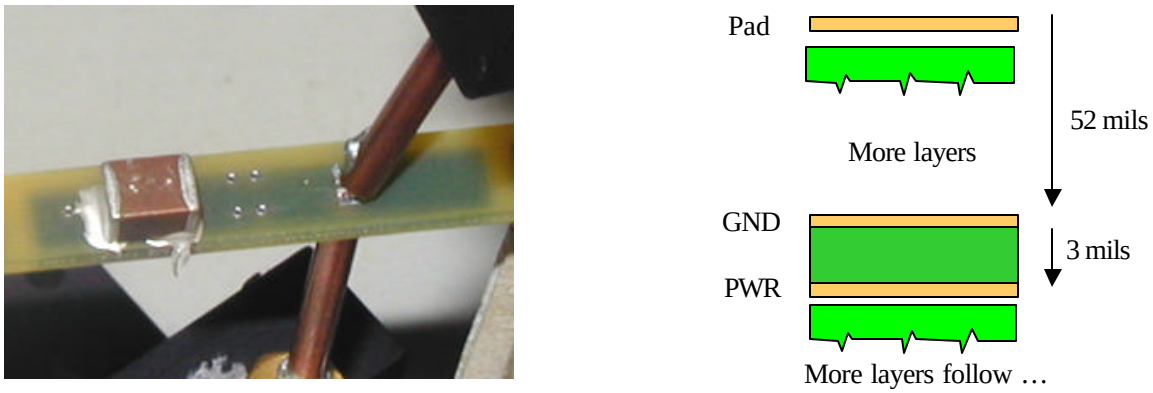

Figure 33: Test Fixture E. On the left: photo of the fixture with a sample capacitor attached with uncured silver-filled epoxi and the two semi-rigid probes for instrument connections. On the right, the stackup of fixture planes is shown. The identical-shape ground and power planes have the size of 955x145 mils. The via length connecting the 75x95-mil capacitor pads to the planes is 52 mils. There are two vias with outward escape from the pads, with a center-to-center spacing of 245 mils.